Is a Crystal Engineering Approach Useful in Designing Metallogels? A Case Study

ARTICLE *in* CRYSTAL GROWTH & DESIGN · OCTOBER 2010

Impact Factor: 4.89 · DOI: 10.1021/cg101078f

3 AUTHORS, INCLUDING:

Nayarassery Narayanan Adarsh
Catalan Institute of Nanoscience and Nanot…
46 PUBLICATIONS **762** CITATIONS
SEE PROFILE

Pathik Sahoo
National Institute for Materials Science
15 PUBLICATIONS **234** CITATIONS
SEE PROFILE

DOI: 10.1021/cg101078f

CRYSTAL GROWTH & DESIGN Article

2010, Vol. 10
4976–4986

Is a Crystal Engineering Approach Useful in Designing Metallogels? A Case Study

N. N. Adarsh, Pathik Sahoo, and Parthasarathi Dastidar*

Department of Organic Chemistry and Centre for Advanced Materials, Indian Association for the Cultivation of Science (IACS), 2A&2B, Raja S. C. Mullick Road, Jadavpur, Kolkata 700032, West Bengal, India

Received August 17, 2010; Revised Manuscript Received September 21, 2010

ABSTRACT: A crystal engineering based design strategy for metallogels has been demonstrated in a series of mixed ligand based Cu^{II}/Co^{II} coordination polymers derived from two bis-pyridyl-bis-amide ligands namely *N*,*N*′-bis-(3-pyridyl)-isophthalamide (**L1**) and *N*,*N*′-bis-(3-pyridyl)terephthalamide (**L2**) and various dicarboxylates. These mixed ligand coordination polymers are shown to form gels as well as X-ray quality crystals under different conditions. The crystal structures of the gel fibers in the xerogels have been determined by using powder and single-crystal X-ray diffraction data. The results support the proof of the concept based on which the metallogels are designed.

Introduction

A supramolecular gel is a viscoelastic material that is formed when a solution containing a small amount of gelator molecule (often known as low molecular weight organic gelator or LMWG having a molecular mass typically < 3000) is cooled below a critical temperature.[1] A metallogel[2] is a special class of supramolecular gel that is formed when solvent molecules are immobilized within a gel network derived from molecules containing metal atoms. The gelling agent could be a discrete metal coordination complex,[3] well-defined coordination polymer,[4] or cross-linked coordination polymer.[5] The term metallogel is being used to emphasize the essential role of metal−ligand bonds in gel network formation.[6] Other classes of metal-containing gel systems are also known; noncoordinating metal ions or metal nanoparticles can be incorporated in the gel matrix, which can act as growth regulators for the preparation of metallic nanoparticles or as templates for the formation of porous or nanoimprinted supramolecular assemblies.[7] The presence of metal ions has also been shown to have drastic effects on the morphology and kinetics of gel formation.[8]

Metallogels are increasingly becoming important as they offer potential applications in catalysis,[9] sensing,[10] photophysics,[11] magnetic materials,[12] etc. However, designing a metallogelator is challenging. Nevertheless, there have been some attempts to design metallogelators that include appending an aromatic-linker-steroid (ALS) (a well-known gel forming fragment) to an organometallic moiety,[13] introducing a long alkyl chain on coordination complex,[14] aborting crystallization by increasing the randomness of mixed ligand carboxylates of Ag^{I} coordination compounds,[15] flexible ligand coordination and slow formation of coordination polymers,[16] and the supramolecular synthon approach.[17]

In this paper, we report an alternative designing approach for metallogelators that is inspired by the intriguing analogies that exist between gels and solvent-occluded crystalline solids; in both the cases, large quantities of solvent molecules are trapped in the corresponding networks that are formed by supramolecular assembly of molecules. In fact, we[18] and others[19] have shown that the single-crystal structures of some gelator molecules capable of gelling highly polar solvents or mixtures of solvents, such DMSO, DMF, water, ethylene glycol, and their various mixtures, contain a large amount of lattice-occluded solvents. Thus, combination of structural features typical of gelators and networks capable of forming crystalline molecular solids having lattice-occluded solvent molecules may be explored to design new metallogelators.

Scheme 1

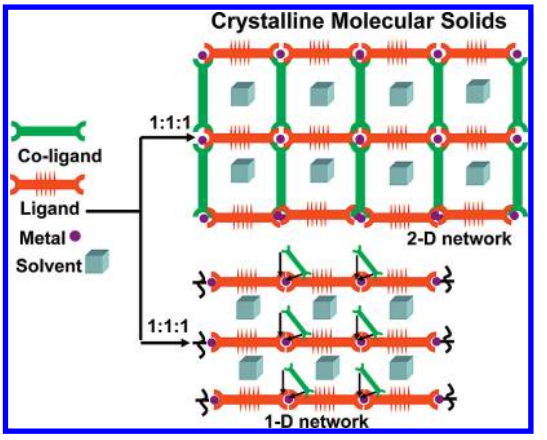

For this purpose, we have reacted separately two bis-pyridyl-bis-amide ligands, **L1** and **L2**, with various dicarboxylates (oxalate, malonate, terephthalate, and napthhthalate) and Cu^{II}/Co^{II} metal centers, respectively, in 1:1:1 (ligand : carboxylate : metal) molar ratio; depending on the coordination modes of the dicarboxylates (either bridging or chelating), both 2-D and 1-D coordination polymeric networks may be formed. The solvent molecules may be occluded within the 2-D grid or within the interstitial space between the 2-D layers. In the case of 1-D chains, the solvent molecules may still be occluded within the lattice assisted by hydrogen-bonding interactions with the ligand backbone (Scheme 1). Thus, it is noted here that the structural features typical of gelators such as conformational flexibility, hydrogen bonding (both present in the ligand **L1** and **L2**) and networks capable of occluding solvent molecules in the crystal lattice are present in these chosen systems.

*To whom correspondence should be addressed. E-mail: parthod123@rediffmail.com; ocpd@iacs.res.in.

Published on Web 10/12/2010

Scheme 2

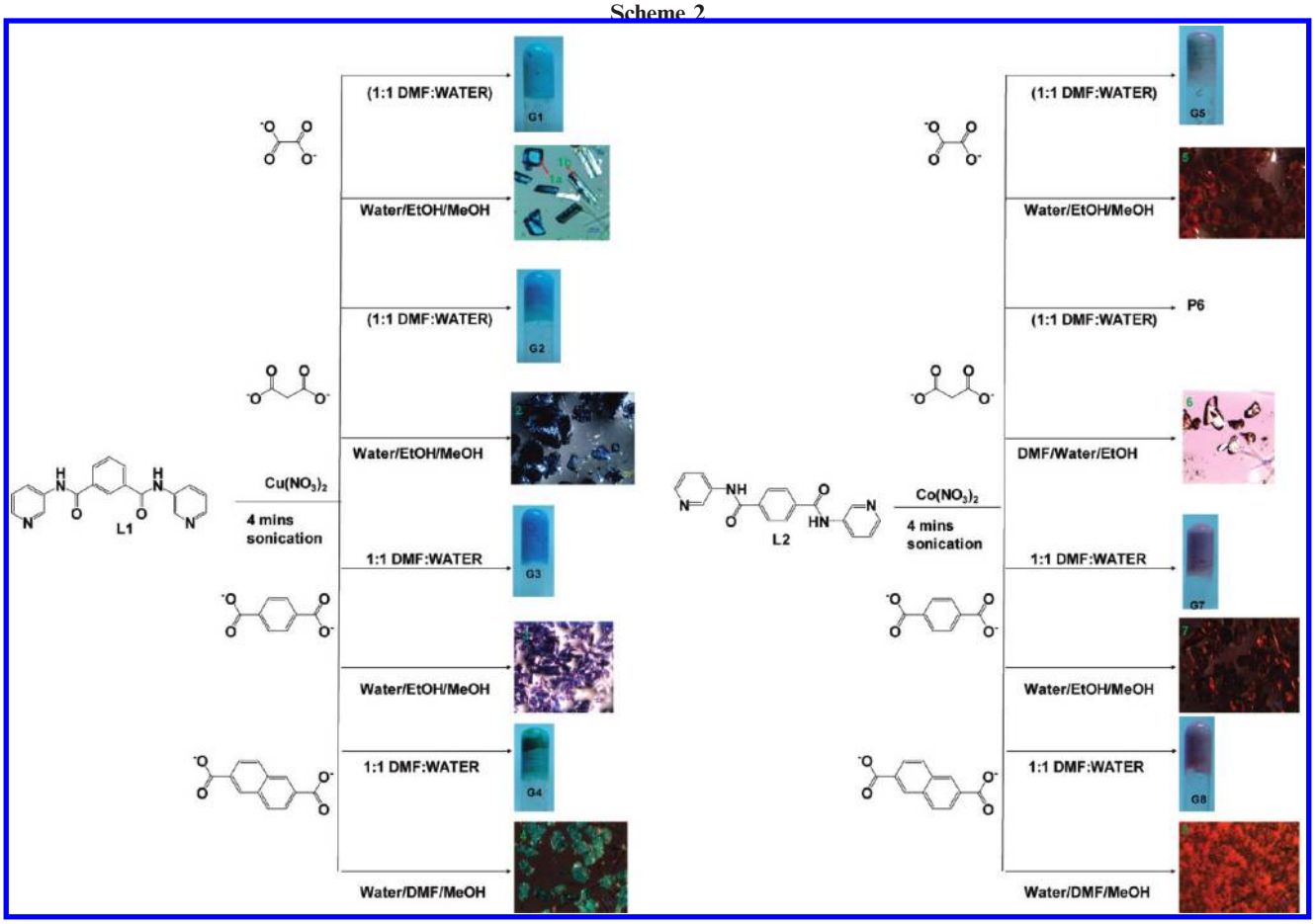

Table 1. Gelation Data[a]

gel	metal salt	pyridyl ligand	carboxylate ligand	minimum gelator concentration (MGC) (wt %)
G1	$Cu(NO_3)_2$ (46 mg, 0.19 mmol)	**L1** (60 mg, 0.19 mmol)	disodium oxalate (25.46 mg, 0.19 mmol)	6.6
G2	$Cu(NO_3)_2$ (53.24 mg, 0.22 mmol)	**L1** (70 mg, 0.22 mmol)	disodium malonate (39.6 mg, 0.22 mmol)	8.1
G3	$Cu(NO_3)_2$ (53.24 mg, 0.22 mmol)	**L1** (70 mg, 0.22 mmol)	disodium terephthalate (53.24 mg, 0.22 mmol)	8.8
G4	$Cu(NO_3)_2$ (53.24 mg, 0.22 mmol)	**L1** (70 mg, 0.22 mmol)	disodium naphthalate (64.24 mg, 0.22 mmol)	9.4
G5	$Co(NO_3)_2$ (55 mg, 0.19 mmol)	**L2** (60 mg, 0.19 mmol)	disodium oxalate (25.46 mg, 0.19 mmol)	7.0
G7	$Co(NO_3)_2$ (64 mg, 0.22 mmol)	**L2** (35 mg, 0.11 mmol)	dipotassium terephthalate (53.24 mg, 0.22 mmol)	7.6
G8	$Co(NO_3)_2$ (64 mg, 0.22 mmol)	**L2** (70 mg, 0.22 mmol)	dipotassium naphthalate (64.24 mg, 0.22 mmol)	9.9

[a] A mixture of DMF−H_2O solution (1 mL DMF and 1 mL H_2O) was used for gelation experiments; the relatively high MGC could be due to the rigid nature of the coordination network (*vide infra*); this explanation may be further supported by the fact that at relatively lower concentration, crystals were obtained. However, with the increase in concentration, weak gel-like precipitates and finally gels were obtained.

Results and Discussion

Gelation Studies. It has been found that both **L1** and **L2** could gel 1:1 DMF/water (as concluded based on tube inversion test) when they were reacted with Cu^{II} and Co^{II}, respectively, in the presence of various dicarboxylates in a sonication bath (Scheme 2); the overall concentration of 7−10 wt % (w/v) (considering all the reactants) and a brief sonication are required to effect gelation (Table 1, Figure 1).

The gels were not thermoreversible indicating the coordination polymeric nature of the gel network; the gels were stable under ambient conditions for more than a week except **G2**, which turned into crystals within 24 h. Microscopic observation of the xerogels under a scanning electron microscope (SEM) revealed the presence of relatively short fibers in **G1**, **G3**, and **G5**, and highly entangled fibrious networks in **G2**, **G4**, **G7**, and **G8** (Figure 2). We also separately tested the gelation properties of the ligands. It was observed that both **L1** and **L2** were capable of gelling DMF/water mixture. While the gel derived from **L1** was thermoreversible, the corresponding gel from **L2** did not display thermoreversibility because of its poor solubility in water (Supporting Information).

To characterize the gels further, rheological response using dynamic rheology was tested for some selected gels. All these gels studied for rheology displayed typical gel-like rheological response. Note that **G′** is independent of frequency and considerably higher than **G″** over the range of frequencies (Figure 3). Tube inversion, SEM, and rheology data clearly indicated that **G1**−**G5**, **G7**, and **G8** were indeed gels.

Structure of the Gel Networks. The next task was to establish the structures of the gelling agents, which would deliver new insights into the designing aspects based on which the present study began. However, it is virtually not possible to determine the single-crystal structure of a gel fiber, which is too tiny to collect single-crystal diffraction data. On the other hand, structure determination using powder X-ray diffraction (PXRD) data has not become a routine exercise yet. Moreover, PXRD data of gel samples suffer from the scattering contribution of the solvent molecules and the less crystalline nature of the gel fibers making it more difficult to solve the structure of the gel network *ab initio*.[20] An alternative approach wherein PXRD of the xerogel is compared with that obtained by simulating the single-crystal data is found to be quite effective although there is no certainty that crystal structure of a gel fiber in its xerogel state truly represents that in a gelled state.[21] A reasonable match of the PXRD of the xerogel with that of simulated one indirectly establishes the structure of the gel fiber in a xerogel.[22] With this background, we tried to crystallize the reaction mixtures as depicted in Scheme 2.

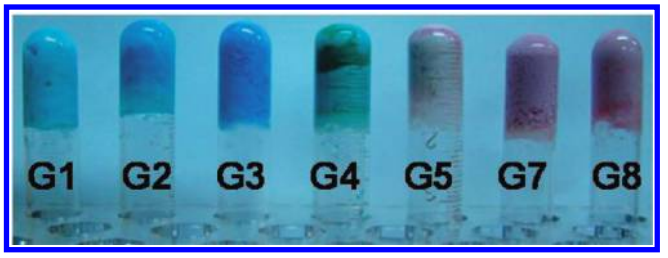

Figure 1. Photographs of various gels reported herein; **G1**−**G5** and **G8** are the corresponding gels as depicted in Scheme 1.

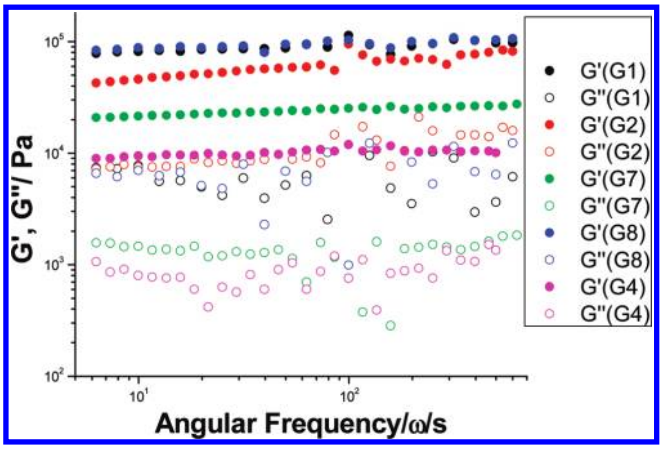

Figure 3. Rheological response of some of the selected gels.

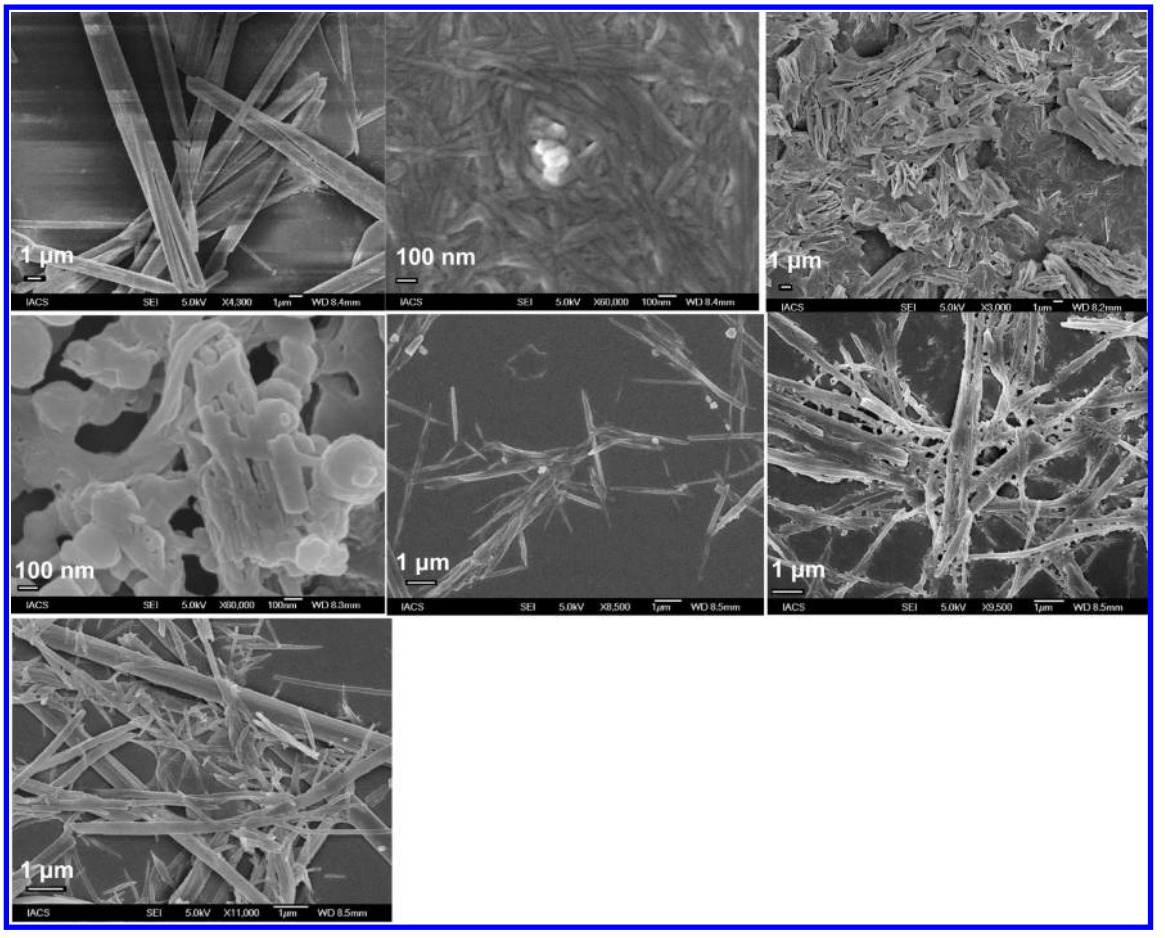

Figure 2. SEM micrographs of the typical fibrous networks of **G1**−**G5**, **G7**, and **G8**.

Table 2. Crystal Data

cryst params	1a	1b	2	3	4	6	7
empirical formula	$C_{20}H_{18}CuN_4O_8$	$C_{20}H_{20}CuN_4O_9$	$C_{21}H_{18}CuN_4O_7$	$C_{26}H_{24}CuN_4O_9$	$C_{36}H_{42}CuN_6O_{12}$	$C_{21}H_{18}CoN_4O_7$	$C_{17}H_{17}CoN_2O_8$
formula weight	505.92	523.94	501.93	600.03	814.30	497.32	436.26
cryst size, mm^3	0.28 × 0.18 × 0.08	0.28 × 0.16 × 0.08	0.32 × 0.22 × 0.08	0.30 × 0.24 × 0.12	0.28 × 0.22 × 0.12	0.24 × 0.14 × 0.07	0.24 × 0.18 × 0.11
cryst syst	monoclinic	monoclinic	monoclinic	monoclinic	triclinic	triclinic	triclinic
space group	$P2_1/n$	$C2/c$	$P2_1/n$	$P2_1/n$	$P\bar{1}$	$P\bar{1}$	$P\bar{1}$
a, Å	13.151(2)	9.282(12)	13.156(4)	10.842(2)	12.1211(5)	5.883(3)	6.344(3)
b, Å	7.9995(13)	26.13(3)	7.855(2)	16.505(3)	13.0168(5)	8.621(4)	9.287(4)
c, Å	18.864(3)	9.799(12)	19.135(5)	14.595(3)	14.4926(5)	12.088(6)	16.008(8)
α, deg	90.00	90.00	90.00	90.00	108.0030(10)	84.727(5)	99.000(5)
β, deg	95.464(4)	109.55(3)	92.521(4)	107.125(3)	98.5860(10)	76.275(5)	96.824(6)
γ, deg	90.00	90.00	90.00	90.00	106.5620(10)	82.535(5)	102.660(6)
vol, $Å^3$	1975.4(6)	2240(5)	1975.5(9)	2496.1(9)	2012.51(13)	589.3(5)	897.4(7)
Z	4	4	4	4	2	1	2
F(000)	1036	1076	1028	1236	850	255	448
μ Mo Kα, mm^{-1}	1.166	1.029	1.162	0.940	0.609	0.775	1.006
temp, K	298(2)	298(2)	298(2)	100(2)	298(2)	298(2)	100(2)
R_{int}	0.0624	0.0648	0.0296	0.0722	0.0424	0.0539	0.0351
range of h, k, l	−14/14, −8/8, −20/20	−9/9, −26/26, −9/9	−15/14, −9/8, −14/22	−11/11, −17/17, −15/15	−14/14, −15/15, −17/17	−6/6, −9/9, −13/13	−7/7, −11/11, −19/19
θ min/max, deg	1.81/23.02	1.56/20.95	1.84/24.99	1.91/22.05	1.53/24.99	1.74/22.81	1.30/25.00
reflns collected/unique/ observed [$I > 2\sigma(I)$]	15192/2750/2176	7051/1198/897	9517/3483/2876	17826/3079/2375	18834/7090/5711	3322/1585/1326	8578/3152/2692
data/restraints/params	2750/0/298	1198/0/155	3483/0/298	3079/0/383	7090/0/481	1585/0/152	3152/6/277
GOF on F^2	1.069	1.132	1.053	1.040	1.033	1.369	1.056
final R indices [$I > 2\sigma(I)$]	R_1 = 0.0397 wR_2 = 0.1058	R_1 = 0.0517 wR_2 = 0.1379	R_1 = 0.0498 wR_2 = 0.1322	R_1 = 0.0359 wR_2 = 0.0822	R_1 = 0.0389 wR_2 = 0.0746	R_1 = 0.1582 wR_2 = 0.3940	R_1 = 0.0350 wR_2 = 0.0911
R indices (all data)	R_1 = 0.0531 wR_2 = 0.1139	R_1 = 0.0683 wR_2 = 0.1456	R_1 = 0.0608 wR_2 = 0.1388	R_1 = 0.0537 wR_2 = 0.0896	R_1 = 0.0502 wR_2 = 0.0781	R_1 = 0.1725 wR_2 = 0.4078	R_1 = 0.0427 wR_2 = 0.0958

For this purpose, we have slowly evaporated a much diluted solution containing the reactants in 1:1:1 molar ratio, which resulted in seven single crystals, **1a**−**7** (Scheme 2), wherein the crystals **1a** and **1b** are concomitantly formed. Single-crystal X-ray diffraction studies revealed that all of them are coordination polymers with the following chemical formula: $[Cu(\mu\text{-}\mathbf{L1})(H_2O)_2(oxalate)]_\infty$ (**1a**), $[\{Cu(\mu\text{-}\mathbf{L1})(\mu\text{-oxalate})\}\cdot 3H_2O]_\infty$ (**1b**), $[Cu(\mu\text{-}\mathbf{L1})(malonate)(H_2O)]_\infty$ (**2**), $[\{Cu(\mu\text{-}\mathbf{L1})(H_2O)_2(\mu\text{-terephthalate})\}\cdot 2H_2O]_\infty$ (**3**), $[\{Cu(\mu\text{-}\mathbf{L1})(H_2O)(\mu\text{-naphthalate})\}\cdot 3H_2O\cdot 2DMF]_\infty$ (**4**), $[\{Co(\mu\text{-}\mathbf{L2})(malonate)\}\cdot H_2O]_\infty$ (**6**), and $[\{Co(\mu\text{-}\mathbf{L2})_{0.5}(H_2O)_2(\mu\text{-terephthalate})\}\cdot H_2O]_\infty$ (**7**). Crystallographic parameters of the coordination polymers reported herein are listed in Table 2. Selected angles and bond distances involving the coordination sphere of the metal center are given in Table 3.

$[Cu(\mu\text{-}L1)(H_2O)_2(oxalate)]_\infty$ (1a) and $[\{Cu(\mu\text{-}L1)(\mu\text{-oxalate})\}\cdot 3H_2O]_\infty$ (1b). When **L1** and dipotassium oxalate were reacted with $Cu(NO_3)_2$ in aqueous MeOH/EtOH mixture (see Experimental Section), two different types of crystalline compounds, blue-colored, block-shaped crystals of **1a** and pale-blue-colored plate -shaped crystals of **1b**, have been isolated. Single-crystal X-ray diffraction experimental analysis revealed that **1a** belonged to the centrosymmetric monoclinic space group $P2_1/n$. The asymmetric unit was comprised of one Cu^{II} metal center, a full molecule of **L1**, an oxalate anion, and two molecules of water (all are coordinated to the Cu^{II} metal center). The Cu^{II} metal center in **1a** is significantly distorted from octahedral geometry as revealed from the corresponding ∠O−Cu—O, ∠O−Cu—N, and ∠N−Cu—N angles [83.18(11)°, 90.12(12)−91.96(13)°, and 95.14(13)°, respectively] (Table 3). The ligand **L1** exhibits significant nonplanarity in **1a** (Table S1, Supporting Information) in the crystal structure. The crystal structure can be best described as a one-dimensional *wavy* coordination polymer formed by the extended coordination of the ligand **L1** (which is in *syn*−*anti*−*syn* conformation, Scheme S1, Supporting Information) with the Cu^{II} metal center. The 1D coordination polymeric chains are further packed in the crystal lattice via various hydrogen-bonding interactions [N···O = 2.934(4)−2.982(4) Å; ∠N−H···O = 153.5−161.6°; O···O = 2.753(5)−3.037(5) Å] (Figure 4).

On the other hand, the crystals of **1b** crystallized in monoclinic $C2/c$ space group. In the asymmetric unit, the metal center, which is located on a center of inversion, is axially coordinated by pyridyl N atom of ligand **L1** and equatorially coordinated by the O atoms of oxalate. The metal center displays a distorted octahedral geometry (Table 3). The extended coordination of the axially coordinated pyridyl ligand **L1** resulted in a 1D zigzag coordination polymer. These polymer chains are further linked via extended coordination by oxalate counteranion resulting in a 2D corrugated sheet (Figure 5). The 2D sheets are further packed in parallel fashion via van der Waals interactions. Lattice-included water molecules are found to be involved in several hydrogen bonds with amide functionality of **L1**, oxalate, and among themselves via N−H···O and O−H···O interactions [N···O = 3.053(9) Å; ∠N−H···O = 162.1°; O···O = 2.701(12)−2.998(11) Å]

$[Cu(\mu\text{-}L1)(malonate)(H_2O)]_\infty$ (2). Dark-blue-colored crystals of **2** crystallized in the centrosymmetric monoclinic space group $P2_1/n$. The asymmetric unit of **2** consists of Cu^{II} metal center, one ligand **L1**, a malonate anion, and a water molecule. In the crystal structure, the Cu^{II} metal center displays distorted square-pyramidal geometry (Table 3). The equatorial positions are occupied by N atoms of two adjacent ligands **L1** and O atoms of malonate. **L1** acts as a bridging ligand, while malonate coordinates to the Cu^{II} metal center in a chelate fashion. The extended coordination of **L1** in its twisted ligating topology (*syn*−*anti*−*syn* conformation, Scheme S1, Supporting Information) with the Cu^{II} metal center resulted in the formation of a 1D coordination

Table 3. Selected Bond lengths (Å) and bond angles (°) involving the coordination geometries of the metal centers

		1a	
Cu(1)−O(25)	1.950(3)	O(25)−Cu(1)−O(29)	83.18(11)
Cu(1)−O(29)	1.973(3)	O(25)−Cu(1)−N(23)	91.96(13)
Cu(1)−N(23)	2.006(3)	O(29)−Cu(1)−N(1)	90.12(12)
Cu(1)−N(1)	2.010(3)	N(23)−Cu(1)−N(1)	95.14(13)
		1b	
Cu(1)−N(1)	2.033(6)	N(1)−Cu(1)−O(14)	89.0(2)
Cu(1)−O(14)	2.075(5)	N(1)−Cu(1)−O(14)	91.03(19)
Cu(1)−O(15)	2.258(5)	N(1)−Cu(1)−O(14)	91.2(2)
		N(1)−Cu(1)−O(14)	88.7(2)
		N(1)−Cu(1)−O(15)	86.5(3)
		N(1)−Cu(1)−O(15)	93.5(3)
		O(14)−Cu(1)−O(15)	78.2(2)
		2	
Cu(1)−O(25)	1.912(2)	O(25)−Cu(1)−O(31)	92.69(11)
Cu(1)−O(31)	1.950(3)	O(31)−Cu(1)−N(21)	87.39(11)
Cu(1)−N(21)	2.017(3)	O(25)−Cu(1)−N(1)	86.93(11)
Cu(1)−N(1)	2.018(3)	N(21)−Cu(1)−N(1)	93.04(12)
		3	
Cu(1)−O(25)	1.969(3)	O(25)−Cu(1)−O(37)	89.90(12)
Cu(1)−O(37)	1.971(3)	O(37)−Cu(1)−O(33)	87.43(12)
Cu(1)−O(33)	1.986(2)	O(25)−Cu(1)−N(1)	89.74(11)
Cu(1)−N(1)	1.996(3)	O(33)−Cu(1)−N(1)	92.36(11)
Cu(1)−N(23)	2.269(3)	O(25)−Cu(1)−N(23)	87.06(11)
		O(37)−Cu(1)−N(23)	91.88(12)
		O(33)−Cu(1)−N(23)	98.39(11)
		N(1)−Cu(1)−N(23)	94.01(12)
		4	
Cu(1)−O(25)	1.9468(16)	O(25)−Cu(1)−O(41)	90.88(8)
Cu(1)−O(35)	1.9511(16)	O(35)−Cu(1)−O(41)	88.14(8)
Cu(1)−O(41)	1.9847(19)	O(25)−Cu(1)−N(21)	91.42(7)
Cu(1)−N(21)	2.019(2)	O(35)−Cu(1)−N(21)	89.40(7)
Cu(1)−N(1)	2.297(2)	O(25)−Cu(1)−N(1)	90.90(7)
		O(35)−Cu(1)−N(1)	89.68(7)
		O(41)−Cu(1)−N(1)	91.73(7)
		N(21)−Cu(1)−N(1)	102.13(8)
		6	
Co(1)−O(13)	2.015(16)	O(13)−Co(1)−O(19)	96.6(5)
Co(1)−O(17)	2.067(15)	O(13)−Co(1)−O(19)	83.4(5)
Co(1)−N(1)	2.187(11)	O(13)−Co(1)−N(1)	89.9(4)
		O(13)−Co(1)−N(1)	90.1(4)
		O(19)−Co(1)−N(1)	91.4(4)
		O(19)−Co(1)−N(1)	88.6(4)
		7	
Co(1)−O(25)	2.018(2)	O(25)−Co(1)−O(19)	99.43(10)
Co(1)−O(19)	2.052(2)	O(25)−Co(1)−O(26)	83.49(8)
Co(1)−O(26)	2.140(2)	O(19)−Co(1)−O(26)	90.86(8)
Co(1)−O(14)	2.1678(19)	O(25)−Co(1)−O(14)	95.29(9)
Co(1)−O(13)	2.173(2)	O(26)−Co(1)−O(14)	90.49(8)
Co(1)−N(1)	2.174(2)	O(19)−Co(1)−O(13)	104.88(8)
		O(26)−Co(1)−O(13)	85.87(7)
		O(25)−Co(1)−N(1)	93.53(9)
		O(19)−Co(1)−N(1)	88.86(8)
		O(13)−Co(1)−N(1)	97.16(8)
		O(14)−Co(1)−N(1)	90.55(8)

polymer (Figure 6). Such 1D coordination polymers are involved in hydrogen-bonding interactions with each other. While the amide functionality present in **L1** is engaged in hydrogen bonding with the malonate [N···O = 3.010(4)−3.244(4) Å; ∠N−H···O = 153.5−158.2°], the metal-bound water molecule is involved in hydrogen bonding with amide C=O and malonate [O···O = 2.848(4)−2.934(5) Å] (Figure 6).

[{**Cu(*μ*-L1)(H$_2$O)$_2$(*μ*-terephthalate)**}·**2H$_2$O**]$_\infty$ **(3).** Violet-colored, plate-shaped crystals of **3** crystallized in the centrosymmetric monoclinic space group $P2_1/n$. The asymmetric unit of **3** consists of the Cu^{II} metal center, one molecule of ligand **L1**, one terephthalate anion, and a water molecule (all three are coordinated to the metal center), and two molecules of lattice-included water. The Cu^{II} metal center displays distorted square pyramidal geometry (Table 3). In the crystal structure, both **L1** and terephthalate act as bridging ligands; the extended coordination of **L1** with its *syn*−*syn*−*syn* conformation (Scheme S1, Supporting Information) leads to the formation of a right-handed helical chain (Figure 7). The twisted ligating topology of **L1** due to its nonplanarity and *syn*−*syn*−*syn* conformation is the main driving force for the helix formation. Such helical chains are cross-linked by the topologically linear ligand terephthalate resulting in the formation of a two-dimensional corrugated sheet architecture (Figure 7). Such corrugated sheets are packed on top of each other in an offset fashion mediated by hydrogen-bonding interactions involving amide functionality, terphthlate, metal-bound water, and lattice-included water molecules via N−H···O[N···O=2.783(4)−2.915(4) Å; ∠N−H···O = 137.5−168.8°] and O−H···O interactions molecule [O···O = 2.624(4)−3.026(5) Å; ∠O−H···O = 136(4)−173(5)°] (Figure 7).

[{**Cu(*μ*-L1)(H$_2$O)(*μ*-naphthalate)**}·**3H$_2$O·2DMF**]$_\infty$ **(4).** Green-colored, block-shaped crystals of **4** crystallized in the centrosymmetric triclinic space group $P\bar{1}$. In the asymmetric unit of **4**, the Cu^{II} metal center, one molecule of **L1**, one naphthalate anion, one water molecule (all are coordinated to Cu^{II} metal center), and two molecules of lattice-included DMF were present. The Cu^{II} metal center displays distorted square-pyramidal geometry (Table 3). In the crystal structure, both **L1** and naphthalate act as bridging ligands; the extended coordination of **L1** with its *anti*−*anti*−*anti* conformation (Scheme S1, Supporting Information) leads to the formation of a 1D coordination polymer (Figure 8). Such 1D chains are cross-linked by the topologically linear ligand naphthalate resulting in the formation of a two-dimensional corrugated sheet architecture (Figure 8). Such corrugated sheets are packed on top of each other in an offset fashion mediated by hydrogen-bonding interactions involving naphthalate and metal-bound water molecules [O···O = 2.665(3)−2.679(3) Å; ∠O−H···O = 163(3)−178(3)°]. DMF molecules of crystallization were present within the interstitial space between two corrugated sheets and are involved in hydrogen bonding with the amide functionality of **L1** [N···O = 2.820(3)−2.850(3) Å; ∠N−H···O = 158.2−163.87°].

[{**Co(*μ*-L2)(malonate)**}·**H$_2$O**]$_\infty$ **(6).** Pale-pink-colored, plate-shaped crystals of **6** crystallized in the centrosymmetric triclinic space group $P\bar{1}$. In the asymmetric unit of **6**, half-occupied Co^{II} metal, half-occupied ligand **L2**, half-occupied malonate, and half-occupied lattice-included water molecule, all located on or around an inversion center, were present. In the crystal structure, **L2** acts as a bridging ligand, while malonate forms a chelate with Co^{II}. The extended coordination of **L2** with its *syn*−*anti*−*syn* conformation (Scheme S2, Supporting Information) leads to the formation of a 1D zigzag coordination polymer (Figure 9). Such 1D coordination polymers recognize each other by amide−amide hydrogen bonding [N···O = 2.95(3) Å; ∠N−H···O = 163.5°]. Lattice-included water molecules were trapped within the interstitial space and are involved in hydrogen bonding with the amide functionality of the ligand **L2** [O···O = 2.94(4) Å] and malonate [O···O = 2.936(2) Å].

[{**Co(*μ*-L2)$_{0.5}$(*μ*-terephthalate)$_{0.5}$(*μ*-terephthalate)$_{0.5}$(H$_2$O)$_2$**}·**(H$_2$O)**]$_\infty$ **(7).** Pink-colored, block-shaped crystals of **7** crystallized in the centrosymmetric triclinic $P\bar{1}$ space group, and the asymmetric unit consists of one Co^{II} metal center, half-occupied

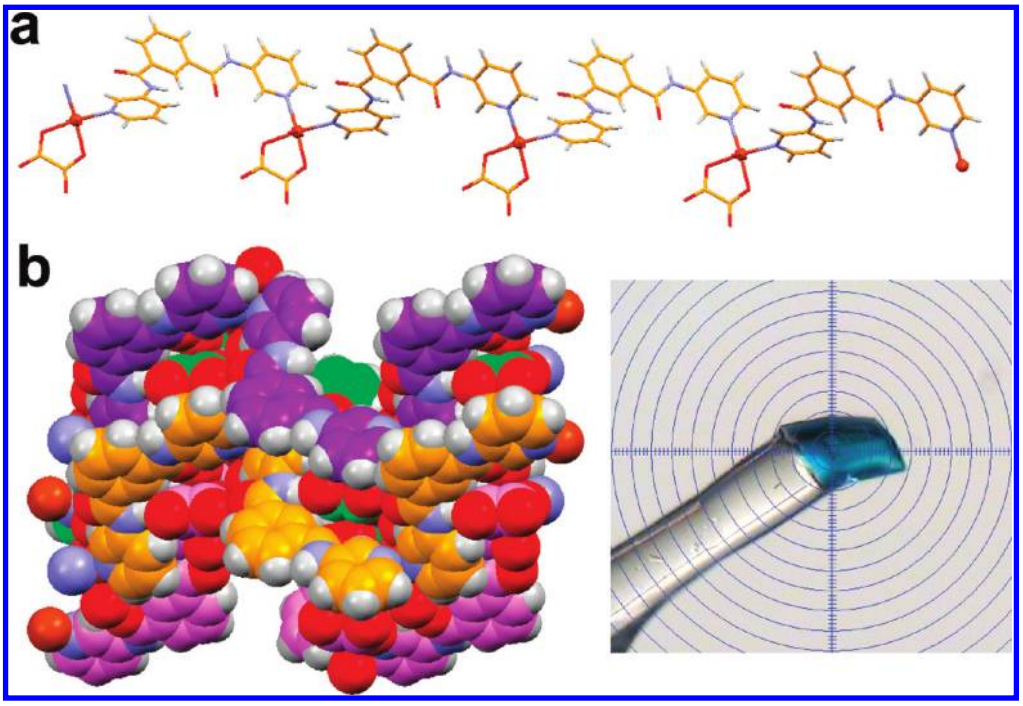

Figure 4. Crystal structure illustration of **1a**: (a) 1D coordination polymer; (b) overall packing of the polymeric chains; inset, the block shaped crystal of **1a** mounted for X-ray diffraction.

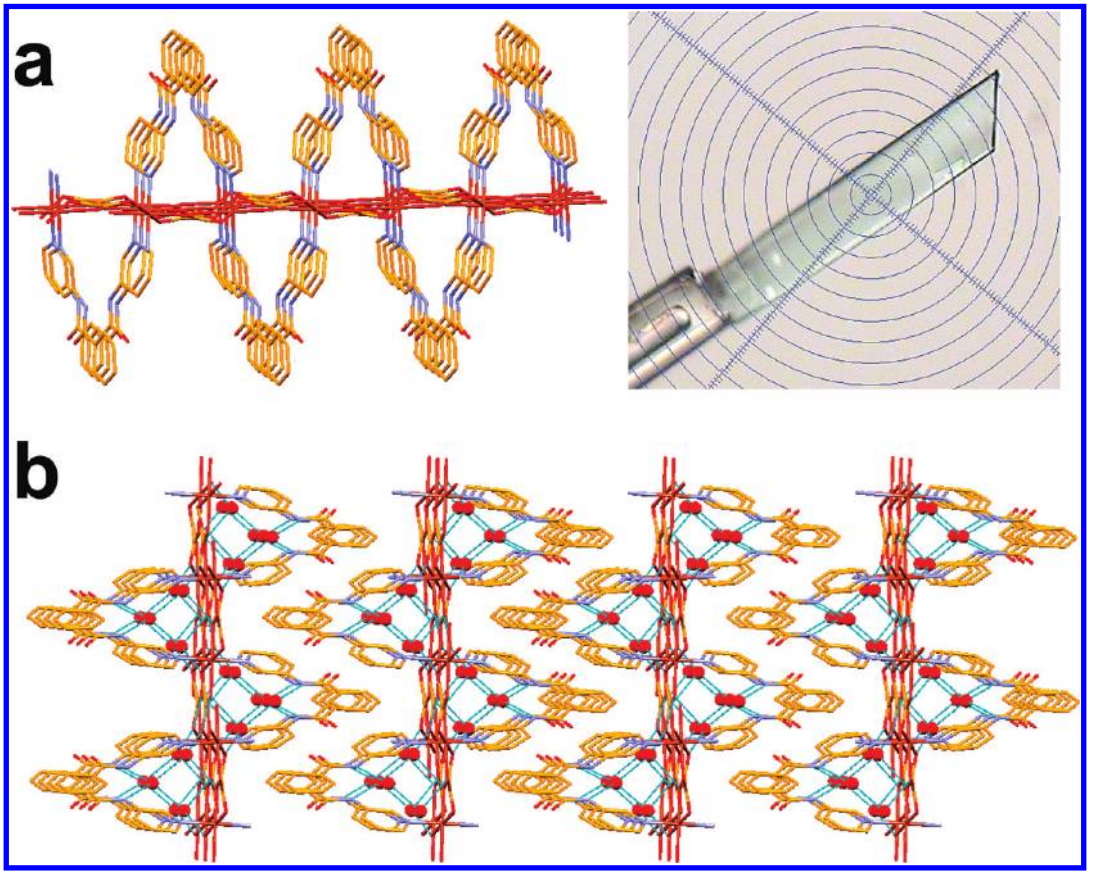

Figure 5. Crystal structure illustration of **1b**: (a) 2D corrugated sheet; (b) parallel packing of 2D sheets and various hydrogen-bonding interactions involving lattice-included water molecules; inset, the plate shaped crystal of **1b** mounted for X-ray diffraction.

ligand **L2**, two half-occupied crystallographically independent terephthalates, two metal-bound water molecules and one lattice-included water. The central aromatic ring of **L2** and terephthalate ions were located on an inversion center. In the crystal structure, the Co^{II} metal center displays distorted octahedral geometry (Table 3). The angular ligating topology of **L2** due to its *anti*−*anti*−*anti* conformation (Scheme S2, Supporting Information), the linear ligating topology of the

crystallographically independent terephthalate ions, and their extended coordination with the Co^{II} metal center leads to the formation of a two-dimensional (6,3) grid architecture (Figure 10). Such 2D sheets are packed on top of each other in an offset fashion supported by hydrogen-bonding interactions involving the amide N−H of **L2** and terephthalate [N···O = 2.818(3) Å; ∠N−H···O = 154.3°] as well as amide C═O of **L2** with the metal-bound water molecule [O···O = 2.708(3)−2.709(3) Å; ∠O−H···O = 166(3)−172(4)°].

The crystal systems of all these crystals are almost evenly distributed between triclinic and monoclinic, wherein the dominant space groups are $P\bar{1}$ and $P2_1/n$, respectively; only **1b** displays the monoclinic space group $C2/c$. The conformational flexibility of both ligands is clearly evident from the various conformations and extent of planarity displayed by these ligands (Supporting Information). In fact, the concomitant formation of **1a** and **1b** appears to be due to the presence of two different conformations of the ligands **L1** (*syn*−*anti*−*syn* and *anti*−*syn*−*anti*, respectively, Scheme S1, Supporting Information) as well as the different coordination modes (chelating and bridging, respectively) of the oxalate. The crystal structures may be categorized into two classes based on the dimensionality of the coordination polymer networks. The crystals of **1a**, **2**, and **6** display 1D coordination polymer chains, whereas the rest of the structures show 2D networks.

The metal : ligand : carboxylate stoichiometry in all the crystal structures is 1:1:1 except in the case of **7** wherein it is 2:1:2; the macrocyclic motif present in this structure contains six Co^{II}, two **L2** and four terephthalates. The requirement for terephthalate at twice the ligand stoichiometry appears to be due to the length of terephthalate, which is just about half the length of the ligand **L2**; as a result, two carboxylates are required to complete the $M_6L_2C_4$ (L = **L2**;

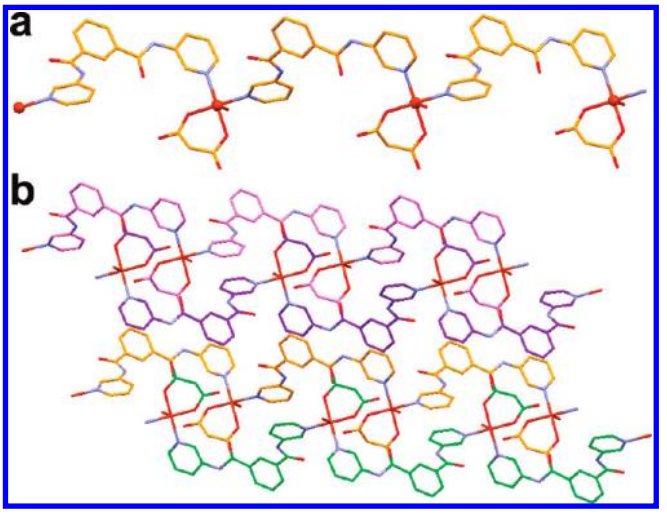

Figure 6. Crystal structure illustration of **2**: (a) 1D coordination polymer; (b) overall packing of 1D coordination network.

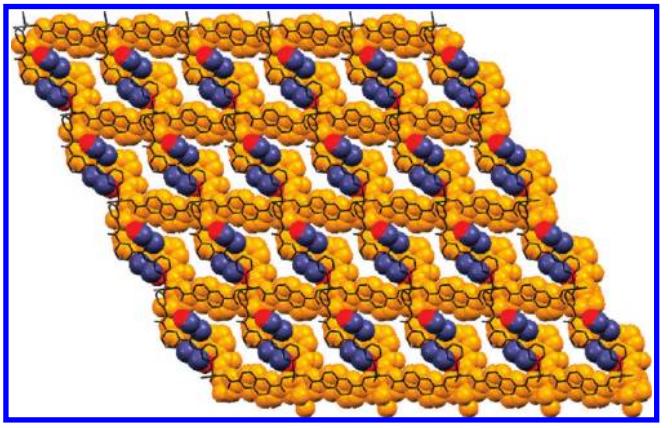

Figure 8. Crystal structure illustration of **4**: offset packing of 2D corrugated sheets (shown in space-filling and capped stick model); lattice-included DMF molecules (shown in space filling model) are occluded between the sheets.

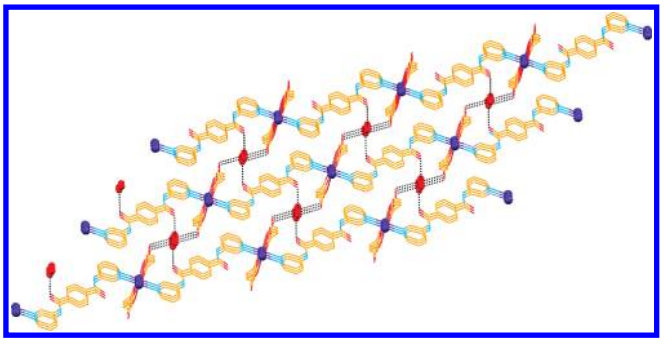

Figure 9. Crystal structure description of **6**: parallel packing of 1D zigzag coordination polymer; disordered water molecules display hydrogen bonding with the amide and malonate.

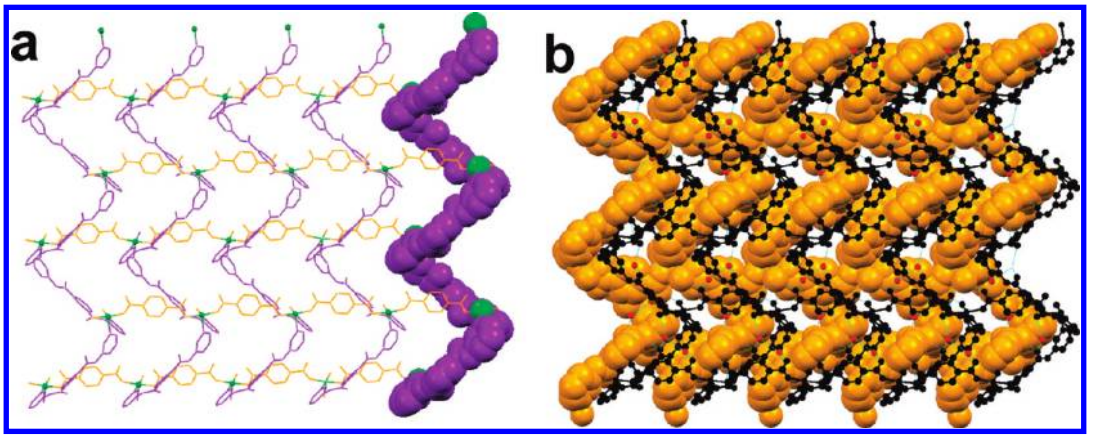

Figure 7. Crystal structure illustration of **3**: (a) 2D corrugated sheet (one right-handed helix is shown in space filling model); (b) offset packing of 2D corrugated sheets (occluded water molecules shown in red color are hydrogen bonded within the network).

C = terephthalate) motif of the 2D grid in **7**. It is interesting to note that all the crystal structures contain lattice-included solvents (water or DMF) and the solvent molecules are hydrogen bonded to the amide backbone of the ligands except **1a** and **2**, which did not have any occluded solvents. FT-IR and elemental analysis data of these crystals and their corresponding xerogels established that the chemical structures of these crystals and that of the corresponding xerogels are same (Figure S1−S7, Table S2, Supporting Information). However, to see whether these crystal structures truly represent the structures of the gel fibers in the corresponding xerogels, PXRD patterns of the bulk solids (i.e., crystallized coordination polymers), xerogels, and the corresponding simulated patterns calculated from the single-crystal X-ray data were compared (Figure 11). It is remarkable to note that the various PXRD patterns of **1b**, **2**, and **4** are nearly superimposable with that of the corresponding simulated patterns thereby elucidating the crystal structures of the gel fibers in the corresponding xerogels. However, the experimental PXRD patterns concerning **G7** and bulk crystals **7** appear to be less crystalline. Nevertheless, the major peaks of these PXRD patterns do match with that in the simulated pattern thereby indicating that the crystalline phases in both the bulk crystals and the xerogel are nearly the same as that of the single-crystal structure of **7**. Poor crystallinity of the bulk as well as xerogel in this case could be due to the

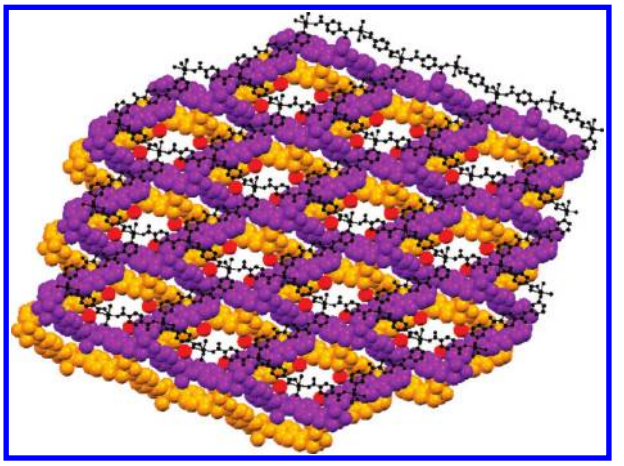

Figure 10. Two-dimensional grid and its offset packing. Occluded solvent water molecules (shown in red, space-filling model) display various hydrogen-bonding interactions within the interstitial space.

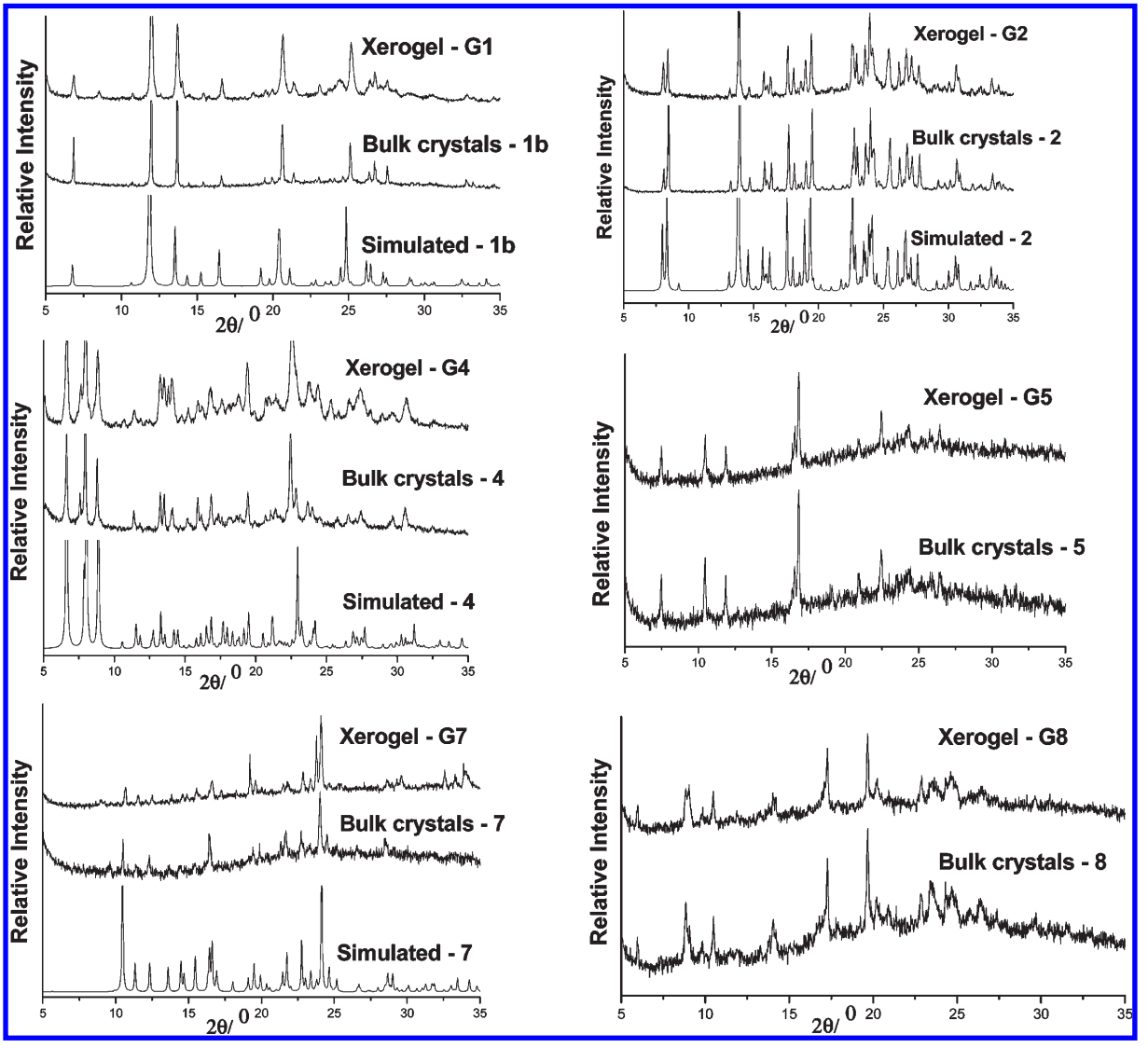

Figure 11. PXRD comparison plots under various conditions.

loss of lattice-included solvents. It is intriguing that the PXRD patterns of the bulk crystals of **5** and **8** also match reasonably well with that of the corresponding xerogels; in the absence of the single-crystal structures of **5** and **8**, it is not possible to comment on the structures of the gel fibers in the xerogels **G5** and **G8**. In the case of **3**, corresponding PXRD patterns did not display good match; since the chemical structure of the **G3** is established based on FT-IR and elemental analysis data (see above), the reason for PXRD mismatch could be the present of other crystalline polymorphs of **3** in the bulk as well as in the xerogel (Supporting Information).

Conclusions

In summary, a crystal engineering based design strategy for metallogels has been demonstrated by discovering a series of metallogelators derived from bis-pyridyl-bis-amide and carboxylate-based mixed ligand systems. These systems are shown to form gels as well as X-ray quality crystals under different conditions. It is remarkable that in the majority of the cases, the PXRD patterns of the xerogels matched well with the corresponding simulated PXRD pattern generated using single-crystal X-ray diffraction data thereby elucidating the structure of the gel fibers in the corresponding xerogels. This case study described herein clearly support the proof of the concept based on which these metallogels are designed.

Experimental Section

Materials and Method. All chemicals were commercially available (Aldrich) and used without further purification. While the ligand *N*,*N*′-bis-(3-pyridyl)isophthalamide, **L1**, was synthesized by following a reported procedure,[23] *N*,*N*′-bis-(3-pyridyl)terephthalamide, **L2**, was previously reported by us[24] and others.[25] The elemental analysis was carried out using a Perkin-Elmer 2400 series-II CHN analyzer. FT-IR spectra were recorded using Perkin-Elmer Spectrum GX, and TGA analyses were performed on a SDT Q Series 600 Universal VA.2E TA Instruments. X-ray Powder Diffraction (XRPD) patterns were recorded on a Bruker AXS D8 Advance Powder (Cu Kα_1 radiation, λ = 1.5406 Å) X-ray diffractometer. Scanning electron microscopy (SEM) was recorded in a JEOL, JMS-6700F, field emission scanning electron microscope. Rheology experiments were performed in an SDT Q series advanced rheometer AR 2000.

Synthesis of the Coordination Polymers 1a−8. 1a and 1b. Coordination polymers [Cu(μ-**L1**)(H_2O)$_2$(oxalate)]$_\infty$ (**1a**) and [{Cu(μ-**L1**)-(μ-oxalate)}·3H_2O]$_\infty$ (**1b**) were concomitantly obtained as blue-colored, block-shaped crystals and pale-blue-colored, plate-shaped crystals, respectively, by layering an ethanolic solution of **L1** (60 mg, 0.19 mmol) over a solution of oxalate (12 mg, 0.09 mmol) in distilled water and later layering a methanolic solution of $Cu(NO_3)_2$ (21.78 mg, 0.09 mmol). The resultant trilayer solution, thus obtained, was kept undisturbed. After 1 week, X-ray quality crystals were obtained. Anal. data calcd for **1a**, $C_{20}H_{18}N_4O_8Cu$: C, 47.48; H, 3.59; N, 11.07. Found: C, 47.74; H, 4.12; N, 11.65. FT-IR (KBr, cm^{-1}): 3400 (m, water O−H stretch), 3259 (m, N−H stretch), 3107, 3093 (s, aromatic C−H stretch), 1678 (s, amide C═O stretch), 1612 (s, amide N−H bend), 1552s, 1485s, 1417s, 1323s, 1307s, 1294s, 1242s, 1195s, 1157m, 1128s, 1099s, 1074m, 1057m, 910s, 881m, 854s, 810s, 796s, 775s, 696s, 653s, 603m, 511m. Anal. data calcd for **1b**, $C_{20}H_{14}N_4O_6Cu.3H_2O$: C, 45.85; H, 3.85; N, 10.69. Found: C, 45.36; H, 3.34; N, 10.48. FT-IR (KBr, cm^{-1}): 3400 (m, water O−H stretch), 3261 (m, N−H stretch), 3161, 3093 (s, aromatic C−H stretch), 1687 (s, amide C═O stretch), 1633s, 1612 (s, amide N−H bend), 1556s, 1485s, 1419s, 1330s, 1323s, 1307s, 1294s, 1242s, 1197m, 1128m, 910w, 808m, 696s.

2. Coordination polymer [Cu(μ-**L1**)(malonate)(H_2O)]$_\infty$ (**2**) was synthesized by layering an ethanolic solution of **L1** (30 mg, 0.094 mmol) over an aqueous solution of dipotassium malonate (8.5 mg, 0.047 mmol) in water and later layering a methanolic solution of $Cu(NO_3)_2$ (11 mg, 0.047 mmol). The resultant trilayer solution, thus obtained, was kept undisturbed. After 1 week, blue, block-shaped X-ray quality crystals were obtained. Anal. data calcd for $C_{21}H_{18}N_4O_7Cu$: C, 50.25; H, 3.61; N, 11.16. Found: C, 49.76; H, 4.20; N, 11.18. FT-IR (KBr, cm^{-1}): 3466 (sb, water O−H stretch), 3292(sb, N−H stretch), 3091w, 3064 (w, aromatic C−H stretch), 1685 (s, amide C═O stretch), 1668s, 1616 (s, amide N−H bend), 1587s, 1548s, 1479s, 1429s, 1329s, 1290s, 1246s, 1193m, 1168m, 1145m, 1128w, 1109w, 1082m, 964m, 931m, 810s, 731s, 719s, 694s, 665m, 648m, 605m, 594m, 578m.

3. Coordination polymer [{Cu(μ-**L1**)(H_2O)$_2$(μ-terephthalate)}·2H_2O]$_\infty$ (**3**) was synthesized by layering an ethanolic solution of **L1** (60 mg, 0.19 mmol) over a solution of dipotassium terephthalate (23 mg, 0.095 mmol) in distilled water and later layering a methanolic solution of $Cu(NO_3)_2$ (23 mg, 0.095 mmol). The resultant trilayer solution, thus obtained, was kept undisturbed. After 1 week, violet, plate-shaped X-ray quality crystals were obtained. Anal. data calcd for $C_{26}H_{20}N_4O_7Cu·2H_2O$: C, 52.04; H, 4.03; N, 9.34. Found: C, 52.28; H, 4.10; N, 10.12. FT-IR (KBr, cm^{-1}): 3412 (sb, water O−H stretch), 3277 (sb, N−H stretch), 3132, 3074 (sb, aromatic C−H stretch), 1672 (s, amide C═O stretch), 1614 (s, amide N−H bend), 1585s, 1546s, 1485s, 1423s, 1423s, 1365s, 1327s, 1298s, 1242s, 1195m, 1101m, 1058m, 1016m, 813m, 802m, 756s, 719s, 698s, 651m, 590w, 528w, 505w.

4. Coordination polymer [{Cu(μ-**L1**)(H_2O)(μ-naphthalate)}·3H_2O·2DMF]$_\infty$ (**4**) was synthesized by layering a DMF−ethanol solution of **L1** (60 mg, 0.19 mmol) over a solution of dipotassium naphthalate (28 mg, 0.095 mmol) in water and later layering a methanolic solution of $Cu(NO_3)_2$ (23 mg, 0.095 mmol). The resultant trilayer solution, thus obtained, was kept undisturbed. After 1 week, green, block-shaped X-ray quality crystals were obtained. Anal. data calcd for $C_{30}H_{22}N_4O_7Cu·3H_2O·2DMF$: C, 53.10; H, 5.20; N, 10.32. Found: C, 53.56; H, 5.42; N, 10.30. FT-IR (KBr, cm^{-1}): 3252 (sb, water O−H stretch), 3132 (sb, N−H stretch), 3093, 3061 (s, aromatic C−H stretch), 1660 (s, amide C═O stretch), 1608 (s, amide N−H bend), 1585s, 1545s, 1485s, 1404s, 1386s, 1357s, 1334s, 1300s, 1290s, 1236s, 1190m, 1136m, 1099m, 1060w, 1047w, 923m, 788s, 717m, 698s, 661w, 650w, 638w, 586w, 478w.

6. Coordination polymer [{Co(μ-**L2**)(malonate)}·H_2O]$_\infty$ (**6**) was synthesized by layering a DMF solution of **L2** (30 mg, 0.094 mmol) over an aqueous solution of dipotassium malonate (8.5 mg, 0.047 mmol) in water and later layering a methanolic solution of $Co(NO_3)_2$ (11 mg, 0.047 mmol). The resultant trilayer solution, thus obtained, was kept undisturbed. After 1 week, pale-pink-colored, block-shaped X-ray quality crystals were obtained. Anal. data calcd for $C_{21}H_{16}N_4O_6Co$: C, 52.62; H, 3.36; N, 11.69. Found: C, 52.80; H, 3.77; N, 11.98. FT-IR (KBr, cm^{-1}): 3427 (sb, water O−H stretch), 3250 (m, N−H stretch), 3099sb, 3039 (sb, aromatic C−H stretch), 1658 (s, amide C═O stretch), 1604 (s, amide N−H bend), 1548s, 1537s, 1485s, 1450s, 1384s, 1332s, 1296s, 1236s, 1193s, 1161m, 1118s, 1105s, 1080s, 1055s, 1020s, 889s, 866s, 837m, 806s, 742s, 717s, 700s, 644s, 607m, 569w, 536w, 516m, 437s, 418s.

7. Coordination polymer [{Co(μ-**L2**)(H_2O)$_2$(μ-terephthalate)}·H_2O]$_\infty$ (**7**) was synthesized by layering a DMF solution of **L2** (30 mg, 0.094 mmol) over an aqueous solution of dipotassium terephthalate (11 mg, 0.047 mmol) in water and later layering a methanolic solution of $Co(NO_3)_2$ (11 mg, 0.047 mmol). The resultant trilayer solution, thus obtained, was kept undisturbed. After 1 week, pink, block-shaped X-ray quality crystals were obtained. Anal. data calcd for $C_{17}H_{15}N_2O_7Co·H_2O$: C, 46.80; H, 3.93; N, 6.42. Found: C, 46.90; H, 3.77; N, 6.98. FT-IR (KBr, cm^{-1}): 3527 (sb, water O−H stretch), 3238 (sb, N−H stretch), 3117 (sb, aromatic C−H stretch), 1658 (s, amide C═O stretch), 1612 (s, amide N−H bend), 1554s, 1541s, 1510s, 1483s, 1415s, 1381s, 1329s, 1298s, 1199s, 1016m, 852m, 810m, 744s, 709s, 547m, 515s.

The crystals of **5** and **8** were not suitable for single-crystal X-ray diffraction. However, the elemental analysis data indicated the formation of coordination compounds having metal : ligand : carboxylate as 1:1:1. Their insolubility in common solvents indicates the polymeric nature of the crystals. The dimensionality, that is whether they have a 1D or 2D network, is not certain. Following are the various physicochemical data for **5** and **8**.

Coordination polymer **5** was synthesized by layering a DMF solution of **L2** (30 mg, 0.094 mmol) over an aqueous solution of disodium oxalate (6.3 mg, 0.047 mmol) in water and later layering

a methanolic solution of $Co(NO_3)_2$ (13.6 mg, 0.047 mmol). The resultant trilayer solution, thus obtained, was kept undisturbed. After 1 week, pink-colored aggregates were obtained. Anal. data calcd for $C_{20}H_{14}N_4O_6Co \cdot 2H_2O$: C, 47.92; H, 3.62; N, 11.18. Found: C, 47.80; H, 3.34; N, 8.94. FT-IR (KBr, cm^{-1}): 3342 (sb, water O−H stretch), 3130 (m, N−H stretch), 3085 (sb, aromatic C−H stretch), 1677 (s, oxalate C═O), 1608 (s, amide C═O stretch), 1548 (s, amide N−H bend), 1510s, 1483s, 1427s, 1384s, 1361s, 1332s, 1315s, 1292s, 1120m, 1054w, 1020w, 889w, 864w, 808s, 715m, 700s, 640m, 615m, 513m, 497m, 414w.

Coordination polymer **8** was synthesized by layering a DMF solution of **L2** (30 mg, 0.094 mmol) over an aqueous solution of dipotassium naphthalate (11 mg, 0.047 mmol) in water and later layering a methanolic solution of $Co(NO_3)_2$ (11 mg, 0.047 mmol). The resultant trilayer solution, thus obtained, was kept undisturbed. After 1 week, a pink-colored microcrystalline precipitate was obtained. Anal. data calcd for $C_{30}H_{20}N_4O_6Co \cdot 5H_2O$: C, 52.87; H, 4.44; N, 8.22. Found: C, 52.90; H, 4.40; N, 8.36. FT-IR (KBr, cm^{-1}): 3420 (sb, water O−H stretch), 3315 (sb, N−H stretch), 3062 (sb, aromatic C−H stretch), 1676 (s, amide C═O stretch), 1606 (s, amide N−H bend), 1544s, 1485s, 1427s, 1359s, 1332s, 1294s, 1191m, 1118m, 1101m, 1024w, 800s, 702m, 646w, 482m.

Single-Crystal X-ray Diffraction. Single-crystal X-ray data was collected using Mo Kα (λ = 0.7107 Å) radiation on a SMART APEX II diffractometer equipped with CCD area detector. Data collection, data reduction, structure solution and refinement were carried out using the software package SMART APEX II. All structures were solved by direct methods and refined in a routine manner. In most of the cases, non-hydrogen atoms were treated anisotropically. In most cases, hydrogen atom positions were generated by their idealized geometry and refined using a riding model; whenever possible, the hydrogen atoms associated with the lattice-included solvents or metal-coordinated solvents were located and refined. Graphics were generated with MERCURY 2.3.

In the crystal structure of **4**, some of the residual electron densities that could not be modeled were squeezed out using SQUEEZE,[26] which showed 64 electrons per unit cell with a total solvent-accessible area volume of 405.5 $Å^3$. Considering the space group $P\bar{1}$, there were 32 electrons per asymmetric unit, which may be attributed to approximately three lattice-included water molecules. TGA data also supported this observation. The relatively noise-free data, thus obtained, were then used for further crystallographic refinement.

In the crystal structure of **6**, the malonate anion was found to be coordinated to the Co^{II} metal center in a chelating fashion. Since the metal center Co^{II} was located on a center of symmetry, the malonate anion was disordered over this center of symmetry. Thus, the site occupancy factors of the atoms belonging to malonate were assigned as 0.5. However, the malonate moiety could not be refined anisotropically presumably due to the relatively poor quality of the crystals.

Acknowledgment. We thank Department of Science & Technology (DST), New Delhi, India, for financial support. A.N.N. and P.S. thank IACS and CSIR, respectively, for SRF fellowship. Single-crystal X-ray diffraction was performed at CSMCRI, Bhavnagar and the DST-funded National Single Crystal Diffractometer 537 Facility at the Department of Inorganic Chemistry, IACS.

Supporting Information Available: Molecular plots and hydrogen-bonding parameters for **1a**−**7**, Schemes S1 and S2, Table S1, thermogravimetric analysis data of **1b**−**6**, gelation data of **L1** and **L2**, Figure S1−S7, Table S2, and crystallographic data in CIF format. This material is available free of charge via the Internet at http://pubs.acs.org.

Note Added after ASAP Publication. This manuscript was originally published on the web on October 12, 2010 with errors to the affiliation line, Introduction, Table 1, Results and Discussion, and Experimental Section. The corrected version was reposted on October 18, 2010.

References

(1) (a) Dastidar, P. *Chem. Soc. Rev.* **2008**, *37*, 2699. (b) George, M.; Weiss, R. G. *Acc. Chem. Res.* **2006**, *39*, 489. (c) Terech, P.; Weiss, R. G. *Chem. Rev.* **1997**, *97*, 3133. (d) Abdallah, D. J.; Weiss, R. G. *Adv. Mater.* **2000**, *12*, 1237. (e) Sangeetha, N. M.; Maitra, U. *Chem. Soc. Rev.* **2005**, *34*, 821. (f) Pal, A.; Hajra, B.; Sen, S.; Aswal, V. K.; Bhattacharya, S. *J. Mater. Chem.* **2009**, *19*, 4325. (g) Ajayaghosh, A.; Praveen, V. K. *Acc. Chem. Res.* **2007**, *40*, 644. (h) Estroff, L. A.; Hamilton, A. D. *Chem. Rev.* **2004**, *104*, 1201. (i) Banerjee, A.; Palui, G.; Banerjee, A. *Soft Matter* **2008**, *4*, 1430. (j) Saha, A.; Manna, S.; Nandi, A. K. *Chem. Commun.* **2008**, 3732. (k) Pozzo, J.-L.; Clavier, G. M.; Desvergne, J.-P. *J. Mater. Chem.* **1998**, *8*, 2575. (l) Oda, R.; Huc, I.; Candau, S. J. *Angew. Chem., Int. Ed.* **1998**, *37*, 2689. (m) Kishida, T.; Fujita, N.; Sada, K.; Shinkai, S. *J. Am. Chem. Soc.* **2005**, *127*, 7298. (n) King, K. N.; McNeil, A. J. *Chem. Commun.* **2010**, *46*, 3511. (o) Smith, D. K. *Nature Chem.* **2010**, *2*, 162. (p) Llusar, M.; Sanchez, C. *Chem. Mater.* **2008**, *20* (3), 782. (q) Abdallah, D. J.; Weiss, R. G. *Chem. Mater.* **2000**, *12*, 406. (r) Kim, T. H.; Seo, J.; Lee, S. J; Lee, S. S.; Kim, J.; Jung, J. H. *Chem. Mater.* **2007**, *19*, 5815. (s) Chung, J. W.; An, B.-K.; Park, S. Y. *Chem. Mater.* **2008**, *20*, 6750. (t) Trivedi, D. R.; Dastidar, P. *Chem. Mater.* **2006**, *18*, 1470. (u) Dutta, S.; Shome, A.; Debnath, S.; Das, P. K. *Soft Matter* **2009**, *5*, 1607.

(2) (a) Piepenbrock, M-O. M.; Lloyd, G. O.; Clarke, N.; Steed, J. W. *Chem. Rev.* **2010**, *110*, 1960. (b) Fages, F. *Angew. Chem., Int. Ed.* **2006**, *45*, 1680. (c) Lloyd, G. O.; Steed, J. W. *Nat. Chem.* **2009**, *1*, 437. (d) Wei, Q.; James, S. L. *Chem. Commun.* **2005**, 1555. (e) Tam, A. Y-Y.; Wong, K. M-C.; Yam, V. W-W. *Chem.—Eur. J.* **2009**, *15*, 4775. (f) Joshi, S. A.; Kulkarni, N. D. *Chem. Commun.* **2009**, 2341. (g) Leong, W. Lee.; Batabyal, S. K.; Kasapis, S.; Vittal, J. J. *Chem.—Eur. J.* **2008**, *14*, 8822. (h) Ray, S.; Das, A. K.; Banerjee, A. *Chem. Mater.* **2007**, *19*, 1633.

(3) (a) Lopez, D.; Guenet, J.-M. *Macromolecules* **2001**, *34*, 1076. (b) Terech, P.; Gebel, G.; Ramasseul, R. *Langmuir* **1996**, *12*, 4321. (c) Ishi-I, T.; Iguchi, R.; Snip, E.; Ikeda, M.; Shinkai, S. *Langmuir* **2001**, *17*, 5825. (d) Kimura, M.; Muto, T.; Takimoto, H.; Wada, K.; Ohta, K.; Hanabusa, K.; Shirai, H.; Kobayashi, N. *Langmuir* **2000**, *16*, 2078.

(4) Terech, P.; Schaffhauser, V.; Maldivi, P.; Guenet, J. M. *Langmuir* **1992**, *8*, 2104.

(5) Hanabusa, K.; Maesaka, Y.; Suzuki, M.; Kimura, M.; Shirai, H. *Chem. Lett.* **2000**, 1168.

(6) Xing, B.; Choi, M.-F.; Xu, B. *Chem. Commun.* **2002**, 362.

(7) (a) Coates, I. A.; Smith, D. K. *J. Mater. Chem.* **2010**, *20*, 6696. (b) Bhattacharya, S.; Srivastava, A.; Pal, A. *Angew. Chem., Int. Ed.* **2006**, *45*, 2934. (c) Basit, H.; Pal, A.; Sen, S.; Bhattacharya, S. *Chem.—Eur. J.* **2008**, *14*, 6534. (d) Bose, P. P.; Drew, M. G. B.; Banerjee, A. *Org. Lett.* **2007**, *9*, 2489. (e) Vemula, P. K.; Aslam, U.; Mallia, V. A.; John, G. *Chem. Mater.* **2007**, *19*, 138.

(8) (a) Batabyal, S. K.; Leong, W. L.; Vittal, J. J. *Langmuir* **2010**, *26*, 7464. (b) Piepenbrock, M-O. M.; Clarke, N.; Steed, J. W. *Langmuir* **2009**, *25*, 8451. (c) Srivastava, A.; Ghorai, S.; Bhattacharjya, A.; Bhattacharya, S. *J. Org. Chem.* **2005**, *70*, 6574. (d) Sreenivasachary, N.; Lehn, J.-M. *Proc. Natl. Acad. Sci. U.S.A.* **2005**, *102*, 5938.

(9) (a) Escuder, B.; Miravet, J. F. *Chem. Commun.* **2005**, 5796. (b) Escuder, B.; Rodríguez-Llansola, F.; Miravet, J. F. *New J. Chem.* **2010**, *34*, 1044. (c) Liu, Y.-R.; He, L.; Zhang, J.; Wang, X.; Su, C.-Y. *Chem. Mater.* **2009**, *21*, 557. (d) Tu, T.; Bao, X.; Assenmacher, W.; Peterlik, H.; Daniels, J.; Dötz, K. H. *Chem.—Eur. J.* **2009**, *15*, 1853. (e) Huang, J.; He, L.; Zhang, J.; Chen, L.; Su, C.-Y. *J. Mol. Catal., A: Chem.* **2010**, *317*, 97.

(10) Bull, S. R.; Guler, M. O.; Bras, R. E.; Meade, T. J.; Stupp, S. I. *Nano Lett.* **2005**, *5*, 1.

(11) (a) Kishimura, A.; Yamashita, T.; Yamaguchi, K.; Aida, T. *Nat. Mater.* **2005**, *4*, 546. (b) Shirakawa, M.; Fujita, N.; Tani, T.; Kaneko, K.; Shinkai, S. *Chem. Commun.* **2005**, 4149. (c) Kume, S.; Kuroiwa, K.; Kimizuka, N. *Chem. Commun.* **2006**, 2442. (d) Tam, A. Y-Y.; Wong, K. M-C.; Wang, G.; Yam, V. W-W. *Chem. Commun.* **2007**, 2028.

(12) Roubeau, O.; Colin, A.; Schmitt, V.; Clérac, R. *Angew. Chem., Int. Ed.* **2004**, *43*, 3283.

(13) Klawonn, T.; Gansäuer, A.; Winkler, I.; Lauterbach, T.; Franke, D.; Nolte, R. J. M.; Feiters, M. C.; Börner, H.; Hentschel, J.; Dötz, K. H. *Chem. Commun.* **2007**, 1894.

(14) Tam, A. Y-Y.; Wong, K. M-C.; Yam, V. W-W. *J. Am. Chem. Soc.* **2009**, *131*, 6253.

(15) Yoon, S.; Kwon, W. J.; Piao, L.; Kim, S.-H. *Langmuir* **2007**, *23*, 8295.

(16) Xing, B.; Choi, M.-F.; Xu, B. *Chem.—Eur. J.* **2002**, *8*, 5028.

(17) (a) Sahoo, P.; Kumar, D. K.; Trivedi, D. R.; Dastidar, P. *Tetrahedron Lett.* **2008**, *49*, 3052. For reviews on supramolecular synthons

and crystal engineering, see: (b) Desiraju, G. R. *Crystal Engineering: The Design of Organic Solids*; Elsevier: Amsterdam, 1989. (c) Desiraju, G. R. *Angew. Chem., Int. Ed. Engl.* **1995**, *34*, 2311. (d) Desiraju, G. R. *Angew. Chem., Int. Ed.* **2007**, *46*, 8342.

(18) (a) Krishna Kumar, D.; Jose, D. A.; Dastidar, P.; Das, A. *Chem. Mater.* **2004**, *16*, 2332. (b) Krishna Kumar, D.; Jose, D. A.; Das, A.; Dastidar, P. *Chem. Commun.* **2005**, 4059. (c) Adarsh, N. N.; Krishna Kumar, D.; Dastidar, P. *Tetrahedron* **2007**, *63*, 7386.

(19) Lebel, O.; Perron, M.-E.; Maris, T.; Zalzal, S. F.; Nanci, A.; Wuest, J. D. *Chem. Mater.* **2006**, *18*, 3616.

(20) Anderson, K. M.; Day, G. M.; Paterson, M. J.; Byrne, P.; Clarke, N.; Steed, J. W. *Angew. Chem., Int. Ed.* **2008**, *47*, 1058.

(21) Ostuni, E.; Kamaras, P.; Weiss, R. G. *Angew. Chem., Int. Ed.* **1996**, *35*, 1324.

(22) (a) Piepenbrock, M-O. M.; Clarke, N.; Steed, J. W. *Langmuir* **2009**, *25*, 8451. (b) Byrne, P.; Lloyd, G. O.; Applegarth, L.; Anderson, K. M.; Clarke, N.; Steed, J. W. *New. J. Chem.* **2010**, 2261.

(23) Qin, Z.; Jennings, M. C.; Puddephatt, R. J. *Inorg. Chem.* **2003**, *42*, 1956.

(24) Adarsh, N. N.; Dastidar, P. *Cryst. Growth Des.* **2010**, *10*, 483.

(25) Rajput, L.; Singh, S.; Biradha, K. *Cryst. Growth Des.* **2007**, *7*, 2788.

(26) Van der Sluis, P.; Spek, A. L. *Acta Crystallogr.* **1990**, *A46*, 194.